Prediction of the physical response for the two-photon photorefractive effect

E. Castro-Camus and L. F. Magaña

Instituto de Física, Universidad Nacional Autónoma de México, Apartado Postal 20-364, CP 01000, México

Received July 24, 2002

We present a new model for the two-photon photorefractive recording process. We solved the resulting set of nonlinear coupled partial differential equations of the model within a linear approximation of the steady state. We found very good agreement with experimental results. © 2003 Optical Society of America

OCIS codes: 190.5530, 190.4720, 190.4400.

The single-photon photorefractive (PR) effect has proved its technological importance[1] as an extraordinary option for information storage in crystals that can handle much larger densities of information than standard magnetic materials.[2] On the other hand, the single-photon process presents problems during information readout. This happens when one illuminates the material to read the information and, at least partly, erases it. One approach to solving these problems is to reduce to a minimum the reading-beam intensity. However, reducing the intensity makes the reading process difficult. There are methods for fixing holograms, for example, by use of protons, but these methods have the disadvantage of making the information difficult to erase quickly by optical means when desired. The two-photon recording process for PR materials has been extensively studied mainly from the experimental point of view.[3–8] This process is an extraordinary recording option that allows nondestructive reading.

In this Letter we present a model of the two-photon photorefractive effect. This description is based on a band transport model that led to a set of nonlinear coupled partial differential equations. We solve only the equations for the stationary state in the linear approximation to check that the physics behind them is correct, but we are working on the numerical solution to the nonstationary, nonlinear coupled equations. Very few theoretical works have been published on the subject of two-photon recording. The model that we propose is simpler than those reported in Refs. 9 and 10, and after comparing our predictions with the experimental results we found excellent agreement.

The two-photon process requires an intermediate allowed level (IL) that is used to maintain a quantity of excited electrons from the valence band (VB) by photons with energy $\hbar\omega_1$ (gating beam). These electrons are then excited again to the conduction band (CB) by another photon with energy $\hbar\omega_2$ (see Fig. 1). The ω_2 frequency light arrives at the PR material after having been divided into two coherent beams, a reference beam and a carrier beam. The interference of these two beams is recorded in the PR material, producing a spatially dependent charge density that induces a gradient of refractive index in the material.

This recording process is a bit more complicated than the single-photon PR effect but has the advantage of allowing a reading process with no erasure problem as a result of re-excitation of the electrons by the reading beam. Notice that in Eqs. (1)–(5), below, we neglect the hole mobility.

We propose a description of the reading process in terms of the following system of nonlinear partial differential equations:

$$\frac{\partial N^+}{\partial t} = (s_1 I_1 + \beta_1)(N - N^+) - \gamma_1 n_1 N^+ - \gamma n N^+, \tag{1}$$

$$\frac{\partial n_1}{\partial t} = (s_1 I_1 + \beta_1)(N - N^+) + \gamma_2 n(n_{01} - n_1) - \gamma_1 n_1 N^+ - (s_2 I_2 + \beta_2) n_1, \tag{2}$$

$$\frac{\partial n}{\partial t} = (s_2 I_2 + \beta_2) n_1 + \frac{1}{e}\nabla \cdot \mathbf{J} - \gamma n N^+ - \gamma_2 n(n_{01} - n_1), \tag{3}$$

$$\nabla \cdot (\epsilon \epsilon_0 \mathbf{E}) = e(N^+ - n - n_1 - N_A), \tag{4}$$

$$\mathbf{J} = [eD\nabla n + e\mu n\mathbf{E} + \hat{\mathbf{e}}_c p(N^+ - N) I_2], \tag{5}$$

where I_1 and I_2 are the intensities of the gating beam and the interference pattern, respectively. We also include n_{01}, the density of traps in the intermediate state (density of allowed states). γ, γ_1, and γ_2 are the recombination factors of the CB–VB, IL–VB, and CB–IL transitions, respectively; β_1 and β_2 are the thermoionization probability constants for transitions VB–IL and IL–CB, respectively; and, of course, the space–time-dependent variable n_1 is the density of

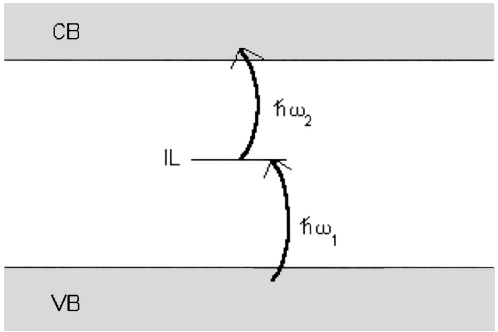

Fig. 1. Transition scheme corresponding to the two-photon photorefractive effect. We consider deep impurity levels and acceptor and donor states that are practically within the VB.

0146-9592/03/131129-03$15.00/0

electrons in the intermediate state. As in the common notation in the literature, e is the electron charge, N is the donor density, N^+ is the density of holes, and n is the density of electrons in the CB. Notice that the presence of the new variable n_1 induces an extra differential equation (2) and more changes in the material rate equations in comparison with the set of single-photon BTM equations proposed by Kuhktarev *et al.*[11]

Equation (1) refers to the time evolution of the VB hole density. Holes can be generated by photoionization and thermoionization, and they disappear when electrons from the IL and the CB are recombined. Equation (2) gives the evolution of the electron density at the IL; this population grows as a result of photoionization and thermoionization from VB and by recombination from CB and decreases by recombination to the VB and by photoionization to the CB. Equation (3) refers to the density of electrons at the CB, which increases because of photoionization and thermoionization from the IL and also because of travel of the electrons in the material; the density decreases because of recombination to the VB and to the IL. We consider deep impurity levels and acceptor and donor states that are practically within the VB (Fig. 1).

First, notice that we can neglect the term $(n_{01} - n_1) \ll N_A$ with respect to the other terms. In the stationary state we take the approximation $N^+ \sim N_A$ and make the time derivatives of N^+, n, and n_1 equal to 0 to find the steady solution, so we get

$$n = \frac{s_1 I_1 s_2 I_2 (N - N_A)}{\gamma N_A (s_2 I_2 + \gamma_1 N_A)}, \tag{6}$$

$$n_1 = \frac{s_1 I_1 (N - N_A)}{s_2 I_2 + \gamma_1 N_A}, \tag{7}$$

$$\frac{\partial}{\partial y}\left(D \frac{\partial n}{\partial y} + \mu n E\right) = 0, \tag{8}$$

and integrating Eq. (8), we get

$$E = \frac{J_0 - D \dfrac{\partial n}{\partial y}}{\mu n}. \tag{9}$$

From Eq. (9) we obtain the expression for the electric field at each point.

Graphs of n, n_1, and E are presented in Figs. 2–4. We take the values shown in Table 1 as the constants. Some of these values were found in the literature, and others were estimated on physical grounds.

In Figure 2 we present n as a function of the spatial coordinate y. One can see that the electrons prefer the darker zones of the material ($\hbar\omega_2$) as expected. From Fig. 3, one can see that the quantity of electrons shows certain structures in which we can find slight oscillations of the order of $10^{15}\,\mathrm{m}^{-3}$ near the value $1.6 \times 10^{20}\,\mathrm{m}^{-3}$, with maxima and minima in the low and high illuminated ($\hbar\omega_2$) areas, respectively (as expected too). We obtained the expected behavior for the space-charge field, which is shown in Fig. 4. This space-charge field follows the normal profile for the light-intensity pattern used.

The refractive index Δn_{ri} is

$$\Delta n_{\mathrm{ri}} = r N_0{}^3 E_{\mathrm{sc}}, \tag{10}$$

where r is the electro-optic coefficient, N_0 is the initial refractive index, and E_{sc} is the magnitude

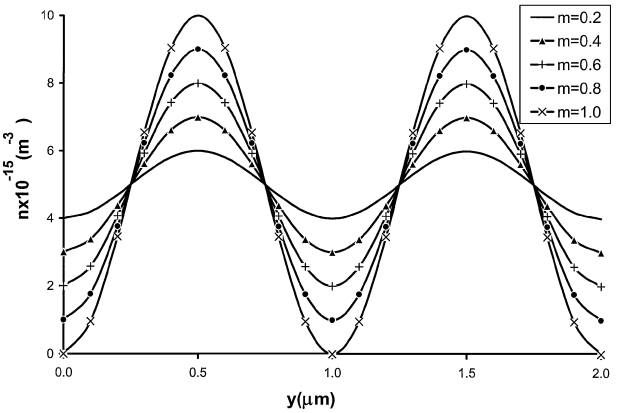

Fig. 2. Density of free electrons (n) in the valence band as a function of the spatial coordinate y.

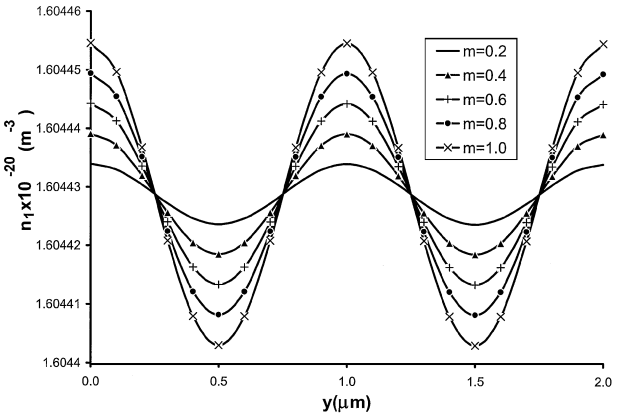

Fig. 3. Density of electrons on the intermediate level (n_1) as a function of the spatial coordinate y.

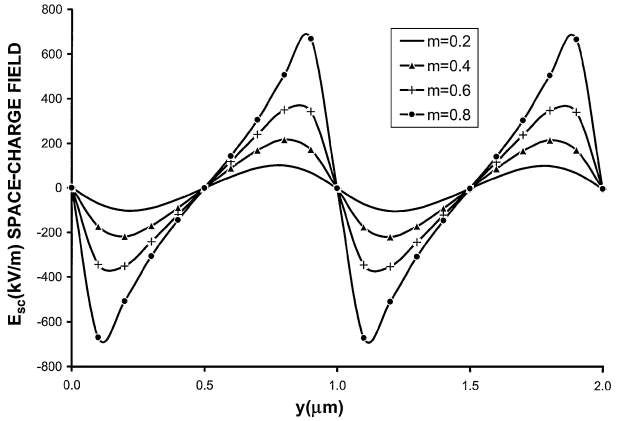

Fig. 4. Space-charge electric field (E_{sc}) as a function of the spatial coordinate y.

Table 1. Constants Used for Our Calculations

Constant	Value	Source[a]
s_1	$1.06 \times 10^{-6}\,\mathrm{m}^2$	Expected
s_2	$1.06 \times 10^{-6}\,\mathrm{m}^2$	Expected
I_0	$5 \times 10^{6}\,\mathrm{W\,m}^{-2}$	Typical[b]
I_1	$5 \times 10^{6}\,\mathrm{W\,m}^{-2}$	Typical[b]
N	$10^{25}\,\mathrm{m}^{-3}$	Typical[c]
N_A	$10^{22}\,\mathrm{m}^{-3}$	Typical[c]
γ_1	$3.3 \times 10^{-17}\,\mathrm{m}^3\,\mathrm{s}^{-1}$	Expected
γ_2	$3.3 \times 10^{-17}\,\mathrm{m}^3\,\mathrm{s}^{-1}$	Expected
γ	$1.65 \times 10^{-17}\,\mathrm{m}^3\,\mathrm{s}^{-1}$	[d]
k	$2\pi/\Lambda$	Typical
μ	$3 \times 10^{-6}\,\mathrm{m}^2\,\mathrm{V}^{-1}\,\mathrm{s}^{-1}$	[c,d]
D	$2.4 \times 10^{-6}\,\mathrm{m}^2\,\mathrm{s}^{-1}$	Typical
β_1	0	Typical
β_2	0	Typical
Λ	$10^{-6}\,\mathrm{m}$	Typical

[a]When available.
[b]Ref. 9.
[c]Ref. 7.
[d]Ref. 6.

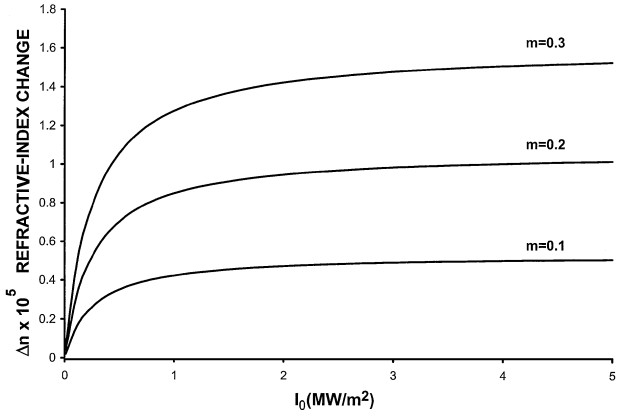

Fig. 5. Change of refractive index as a function of the light ($\hbar\omega_2$) intensity.

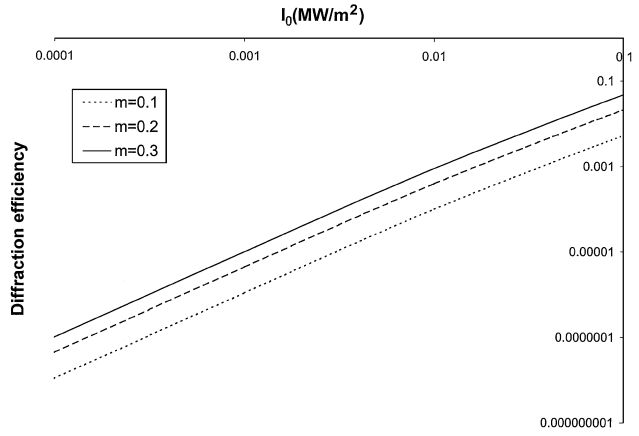

Fig. 6. Diffraction efficiency as a function of the light ($\hbar\omega_2$) intensity for different modulations.

of the space-charge field. Plotting Eq. (10) as a function of the $\hbar\omega_2$ light intensity (I_0), we obtain the result shown in Fig. 5. In the figure one can see an increasing curve that reaches a saturation value. This behavior is the same as that shown in several other experiments.[4,12]

Finally we can analyze the diffraction efficiency, given by the well-known expression

$$\eta = \sin^2\left(\frac{\pi \Delta n_{\mathrm{ri}}}{\lambda \cos\theta_B} L\right),$$

where λ is the recording light wavelength, θ_B is the Bragg angle, and L is the thickness of the sample. From this expression, and using Eq. (10), we get the diffraction efficiency shown in Fig. 6. One can see a family of growing curves that stabilizes for high I_0 values. This behavior is the same as was reported experimentally.[13]

Our model leads to a physically expected behavior for each variable analyzed. In particular, we found very good agreement with available experimental results for the refractive index and diffraction efficiency as a function of light intensity.

We acknowledge funding from the Dirección General de Asuntos del Personal Académico–Universidad Nacional Autónoma de México (project IN118200).
E. Castro-Camus's e-mail address is castro@fisica.unam.mx; L. F. Magaña's is fernando@fisica.unam.mx.

References

1. E. Krätzig and R. Orlowski, Appl. Phys. **15,** 133 (1979).
2. F. Chen, J. LaMacchia, and D. Fraser, Appl. Phys. Lett. **13,** 223 (1968).
3. D. von der Linde, A. Glass, and K. Rodgers, Appl. Phys. Lett. **25,** 155 (1974).
4. H. Vormann and E. Krätzig, Solid State Commun. **49,** 843 (1984).
5. Y. S. Bai and R. Kochru, Phys. Rev. Lett. **78,** 2944 (1997).
6. Y. S. Bai, R. Neurgaonkar, and R. Kochru, Opt. Lett. **22,** 334 (1997).
7. K. Buse, L. Holtmann, and E. Krätzig, Opt. Commun. **85,** 183 (1991).
8. S. Kostritskii, D. Maring, R. Tlavykaev, and R. Ramaswamy, Appl. Opt. **39,** 4292 (2000).
9. L. Paraschis, M. Brashaw, A. Liu, and L. Hesselink, J. Opt. Soc. Am. B **14,** 2670 (1997).
10. T. Nikolajsen, P. Johansen, B. Sturman, and E. Podivilov, J. Opt. Soc. Am. B **18,** 485 (2001).
11. N. Kukhtarev, V. Markov, S. Odoulov, M. Soskin, and V. Vinetskii, Ferroelectrics **22,** 949 (1979).
12. F. Chen, J. Appl. Phys. **40,** 3389 (1969).
13. H. Guenther, G. Wittmann, R. Macfarlane, and R. Neurgaonkar, Opt. Lett. **22,** 1305 (1997).